American Journal of Analytical Chemistry, 2023, 14, 184-201
https://www.scirp.org/journal/ajac
ISSN Online: 2156-8278
ISSN Print: 2156-8251

Modeling of Fixed Bed Adsorption Column Parameters of Iron(II) Removal Using Ferrihydrite Coated Brick

Oscar Allahdin[1,2*], Eric Foto[1], Nicole Poumayé[1,2], Olga Biteman[1], Joseph Mabingui[1], Michel Wartel[2]

[1]UNESCO Chair "Water Management", Lavoisier Hydrosciences Laboratory, University of Bangui, Bangui, Central African Republic
[2]University of Lille 1, LASIR Laboratory (UMR CNRS 8516), Environmental Physicochemistry Research Group, Lille, France
Email: *allahdin25@yahoo.fr

How to cite this paper: Allahdin, O., Foto, E., Poumayé, N., Biteman, O., Mabingui, J. and Wartel, M. (2023) Modeling of Fixed Bed Adsorption Column Parameters of Iron(II) Removal Using Ferrihydrite Coated Brick. *American Journal of Analytical Chemistry*, **14**, 184-201.
https://doi.org/10.4236/ajac.2023.144011

Received: January 24, 2023
Accepted: April 25, 2023
Published: April 28, 2023

Abstract

Fixed-bed operating experimental column conditions were studied to evaluate the performance of brick from Bangui Region (in Central African Republic), coated with iron oxyhydroxide (ferrihydrite) for the removal of iron(II) from aqueous solution. The prediction of theoretical breakthrough profiles using Bohart and Adams sorption model was employed to achieve characteristic parameters such as depth of exchange zone, time required for exchange zone to move vertically, moving rate for the exchange zone and adsorption capacity useful for fixed-bed column reactor was investigated under varying operating conditions. The effects of bed depth and flow rate on iron(II) adsorption were studied. Our finding revealed that the Brick from Bangui Region (in Central African Republic), coated with ferrihydrite was a very efficient media for the removal of Fe(II) ions from water. The experimental data showed that the depth and the moving rate (10.3 ± 0.6 cm) and (0.208 ± 0.006 cm/min) respectively of the exchange zone (adsorption zone) were independent of variability of the height of the adsorbent bed column, however the variations of the flow rate affect the moving rate of the exchange zone. The bed depth service time (BDST) model was used and permitted us to predict the service times of columns operated at various flow rates and bed depths and these predicted values were compared with the experimental values.

Keywords

Iron Oxyhydroxide-Coated Brick, Iron(II)-Adsorption, Column Study, Breakthrough Curve, BDST

1. Introduction

Iron contamination of ground water is widely observed in many countries in the world. There have been numerous reports on iron contamination making potable water increasingly readily unavailable in most countries, and this shortage is most dramatic in developing countries with rapid population growth. Iron is not considered a toxic metal, although its contamination constitutes a serious environmental issue. On the other hand iron(II) in water in contact with air oxygen, is easily oxidized into colloidal ferric oxides/hydroxides, water becomes yellow-ochre with time, making it inappropriate for consumption and for washing clothes [1] [2]. This precipitation further worsens with time bacterial proliferation that causes bad tastes, bad odors and poses the greatest threat to human health.

75% of the subsoil in the CAR is of non-carbonated Precambrian formation, the layers resulting from cracks and faults in this type of subsoil are generally exceeded by a laterite cover, which can promote the loading of the layer by iron due to the slightly acid pH of the waters. The high iron contents were revealed by the intense leaching of the lateritic layers recognized in several areas of the country but also by the transformation of sulfides (pyrite, Fe_2S) reported in the quartz formations of the basement.

The maximum level recommended for drinking water by the World Health Organization (WHO) is 0.3 mg/L and 0.2 mg/L by European Union respectively. This low guideline recommended for maximum iron content in drinking water explains the inconvenience caused by this metal in drinking water.

Moreover, numerous methods had been used in the past years in water purification processes, such as ion exchange on cationic exchange resins [1]; oxidation precipitation by aeration [1] [2]; and adsorption [3]. Among them, the development of water treatment using adsorption processes receives major attention due to its low cost, simplicity and high efficiency.

To improve the quality of iron-contaminated waters, the low cost adsorbents for metal removals have often been preferred particularly, in case the support material (e.g. sand, brick, polymer and sepiolite) was coated with iron oxide/hydroxide [4]-[10]. The sorption performances of these coated materials were found to be dependent upon the quantity of deposited iron oxide/hydroxide; these coatings were higher (than on sands) on brick surfaces because of much greater specific areas due to the presence of metakaolinite [11] [12]. Thus, it was recently shown that: 1) brick from Bangui region (in Central African Republic) possesses high sorption capacity for the removal of soluble iron from aqueous solutions [13]; and 2) freshly precipitated ferric oxyhydroxides on HCl-activated brick contribute to increase significantly Fe(II)-adsorption properties on this material [12] [14] [15]; 3) these cations (Cd^{2+}, Cu^{2+}, Fe^{2+}, Ni^{2+}, Pb^{2+} and Zn^{2+}) were preferentially sorbed by ferrihydrite, rather than other hydroxyl groups in brick clays; 4) adsorption properties of brick for the removal of these divalents cations suggesting the possible implication of electrostatic forces at the brick-

water interface [16].

The aim of this study is to investigate the column performance of iron oxyhydroxide-coated brick and the column operation parameters for the removal of iron(II) from an aqueous solution under dynamic process. Breakthrough studies were carried out to evaluate the performance of iron oxyhydroxide-coated brick in continuous fixed bed operation by varying the operating conditions, such as the flow rate and bed depth. The Bohart and Adams [17] equation was used for the estimation of the basic design parameters characterizing the performance of the dynamic process: such as depth of exchange zone, time required for exchange zone to move vertically, adsorption rate, and adsorption capacity. Theoretically, predicted data points of the column breakthrough curve obtained by using the BDST approach were compared against the experimental breakthrough curve determined in the dynamic process for an initial Fe(II) concentration of 10 mg/L.

2. Materials and Methods

2.1. Preparation of Iron Oxyhydroxydes Coated Brick

Several physical/chemical treatments described by [4] [13] were carried out on the raw brick, briefly: 1) it was broken into grains and sieved to sizes ranging from 0.7 to 1.0 mm; 2) these particles were afterwards leached with a 6 M-HCl solution at 90˚C for 3 h; and 3) finally a deposition of FeOOH on to HCl-treated brick was performed by precipitation of iron(III) by using a 0.25M Fe^{3+} ions solution with NaOH solutions (6 M and 1 M) at pH 7.

2.2. Reagents

All chemicals used for the study were analytical grades of ferric nitrate [$Fe(NO_3)_3$, H_2O], ferrous chloride [$FeCl_2$, $4H_2O$], sodium hydroxide and hydrochloride acid supplied by DISLAB (France). The stock solutions of iron(III) (0.25 mol/L) and iron(II) (10 mg/L) were prepared by dissolving the corresponding salts in Milli-Q water before performing the experiments. It is worth noting that Fe^{2+} ions initially present in the prepared solution (10 mg/L) remained at oxidation state II under our physicochemical conditions (pH ≈ 4.5; Eh = 347 mV vs Ag/AgCl ((KCl) = 3 mol/L)); [O_2] = 5.77 mg/L). Reference electrode has been calibrated whit a redox standard solution (Methrom U (mv) = +250 ± 5 (20˚ pH = 6.994)). The thermodynamic stability of ferrous ions in our solution was further confirmed theoretically by examining the pε-pH diagrams for the iron-water system [18].

3. Instrumentations

3.1. MEB/ESEM/EDS Analyses

Microphotographies of representative brick specimens after precipitation of iron oxyhydroxide were recorded by using an environmental scanning electron microscope (ESEM, Quanta200 FEI). Different surface areas ranging from 0.5 to

3.5 mm^2 were targeted on brick grain sand examined by ESEM/EDS (ESEM, model: QUANTA-200-FEI, equipped with an Energy Dispersive X-Ray Spectrometer EDS X flash 3001 and monitored by QUANTA-400 software elaborated by Bruker). EDS measurements were carried out at 20 kV at low vacuum (1.00 Torr) and the maximum pulse throughput was 20 kcps. Micro-observations along different cross-sections of FeOOH-coated brick samples were also performed by ESEM/EDS.

3.2. XRD Analyses

The powder X-ray diffraction (XRD) was performed by using a Bruker diffractometer (model: Endeavor D4) equipped with a PSD/Lynx Eye detector. The powdered sample was scanned from 10˚ to 8˚ 2θ with increments of 0.0157˚ 2θ and a number of 4456 steps using a Ni-CuKα radiation (the recording time was ≈ 7.2 h). The Cu tube operated at 35 kV and 30 mA. To detect good XRD diffractogram of 2-line ferrihydrite associated with brick, the fraction of brick particles with sizes ≤ 63 μm was recovered and chemically treated according to the procedure described by [14] [15]: A thinner powder was then used in this work to precipitate higher amounts of iron oxyhydroxides on to material surfaces.

3.3. ICP-AES Analyses

ICP-AES (Inductively Coupled Plasma-Atomic Emission Spectroscopy; model Varian Pro Axial View) was used to analyze the soluble iron effluent samples that were collected from the exit of the bottom column at different time intervals.

3.4. Fixed Bed Column Experiments

Continuous flow adsorption according to the experiments described by [13]: was conducted in a fixed-bed glass column with an inner diameter of 14 mm, a height of 30 cm, and a medium porosity sintered-pyrex disk at its bottom in order to prevent any loss of material. Four-bed depths of 10 cm (16 g), 15 cm (23 g), 20 cm (30 g), and 25 cm (38 g) were investigated at a constant flow rate of 10 mL/min, and a constant bed depth of 15 cm was examined at variable rates (3, 5, 8, and 10 mL/min). Before being used in the experiments, 500 ml of Milli-Q water was passed through the column for three reasons: 1) to remove any unbound and thin particles/iron oxides/hydroxides; 2) to check the absence of soluble iron at the outlet; and 3) to confirm the stability of the FeOOH coating on brick pellets. The initial iron(II) concentration of the influent was 10 mg/L. The schematic diagram of the fixed bed column reactor used is shown in (**Figure 1**).

Fe^{2+} ions solution was pumped through the column at a desired flow rate by means of a peristaltic pump (Labo Moderne France Type KD1170) in a downflow mode. Depending upon our various study column experiments, measured pH was found to be around 4.5 in the influent and to vary in the effluent from 8.6 at the beginning to 5.5 at the end. Effluent samples were collected from the

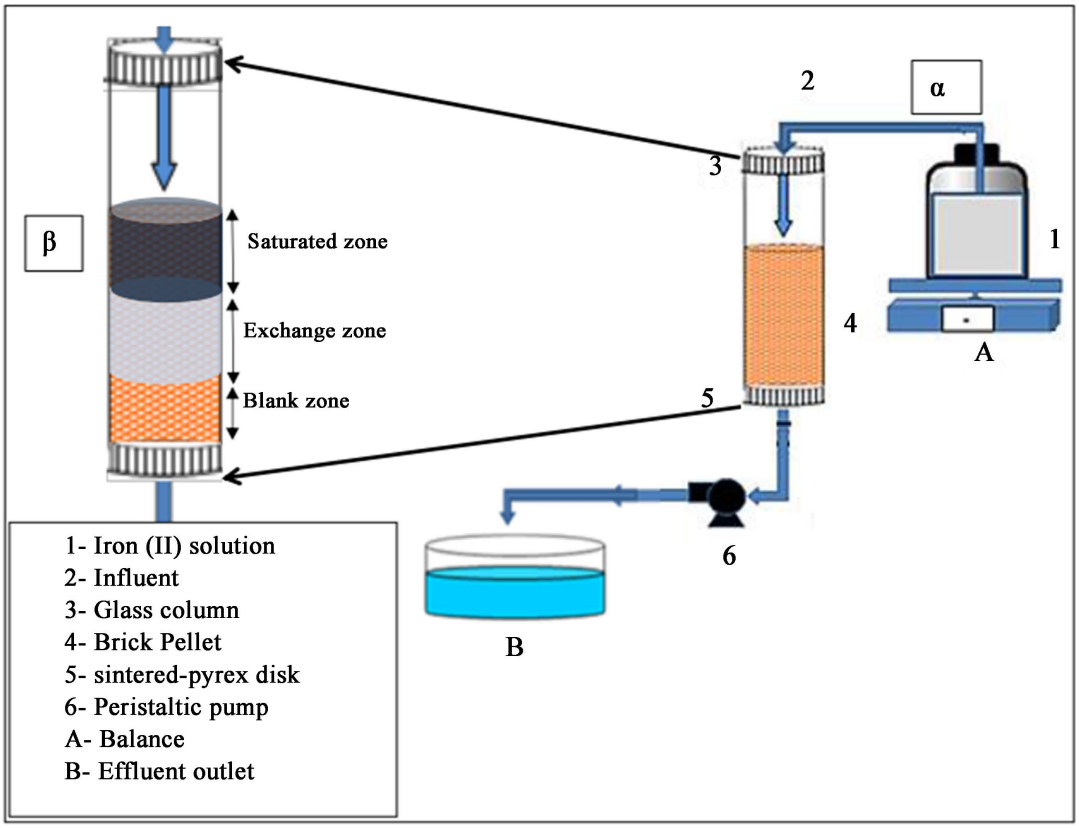

Figure 1. Schematic diagram of the fixed bed column reactor used for Fe(II) adsorption on ferrihydrite coated brick in water.

exit of the bottom column at different time intervals and analyzed for soluble iron using ICP-AES (Inductively Coupled Plasma-Atomic Emission Spectroscopy; model Varian Pro Axial View). The flow to the column was continued until the effluent Fe(II) concentration at time t (C_t) reached the influent Fe(II) concentration (C_0): $C_t/C_0 \approx 0.98$. The performance of packed bed was described in the present work through the concept of the breakthrough curve. The shapes of the breakthrough curves observed during column experiments were studied at variable flow rates and bed depths, and mathematical models were applied to our system.

3.5. Fixed Bed Mathematical Models

The breakthrough time (t_b) corresponding to 5% of initial concentration, the time t50% corresponding to 50% of initial concentration and the exhaust time (t_e) corresponding to the time required to achieve 90% of the inlet concentration were determined. The analysis of the breakthrough curve was done using two models, the prediction of theoretical breakthrough profiles [19] and the bed depth/service time (BDST) model [17]. The BDST model was extended to the prediction of breakthrough and exhaust times of the columns operated at different flow rates and also varied bed height once the slope at a given flow rate and bed height was determined.

4. Results and Discussion

4.1. Composition and Characterization of Ferrihydrite Coated Brick by ESEM/EDS

After deposition of ferrihydrite by precipitation of iron oxyhydroxides on the surface of brick grains according to the procedure described by [13], the micro-observations along different cross-sections of FeOOH-coated brick samples show a deposition of the heterogeneous oxyhydroxides in plate form which is characteristic of gel drying (**Figure 2(a)**).

The profile analysis of the surface of a brick grain after precipitation over a distance of 100 µm (**Figure 2(b)**) shows that iron and silicon are anti-correlated while iron and aluminum are correlated (see **Figure 2(c)**).

This shows that the FeOOH deposited on the grains of the brick adsorbs preferentially on metakaolinite and little on quartz.

4.2. Composition and Characterization of FeOOH Coated Brick by XRD

The raw brick obtained from Bangui region in Central African Republic used in this study was previously characterized by X-ray diffraction and chemical analysis as described before [13] [14] Average mineralogical composition was found to be: 61 - 65 wt% quartz; 21 - 25 wt% metakaolinite; 3 - 4 wt%; illite; ≤ 4 wt%; iron oxides/hydroxides; and ≤2 wt% feldspar + mica + biotite. The XRD analyses of FeOOH-coated brick have been extensively reported in previous studies [13] It shows in the diffractogram of iron oxyhydroxides coated brick two broad maxima at 34˚and 61˚ 2θ corresponding to d-spacings of 1.52˚A and 2.63˚A, typical of two-line ferrihydrite (**Figure 3**).

4.3. Behavior of the Adsorption Column

During the crossing of the column, iron(II) ions are adsorbed on the fixed bed and the solution is exhausted. The iron(II) metal ions in solution are adsorbed at the first adsorbent layer called the exchange zone. During the time $t < t_b$, the outlet concentration of the iron(II) is almost zero. The exchange zone becomes saturated and the exchange zone progressively moves slowly towards the bottom of the adsorbent bed (**Figure 1**). Finally, the exchange zone will reach the bottom of the column at $t = t_b$ and the solute concentration in the outlet effluent begins to increase at $t > t_b$ and reaches its initial value at $t = t_e$.

In order to bring out the fixed bed column, several parameters influencing the breakthrough time were performed to determine the optimal operating conditions of treatment using ferrihydrite-coated brick fixed bed column.

5. Evaluation of the Maximum Capacity of the Fixed Bed

The maximum capacity that represents the total efficiency of a fixed bed can be calculated experimentally using Equation (1):

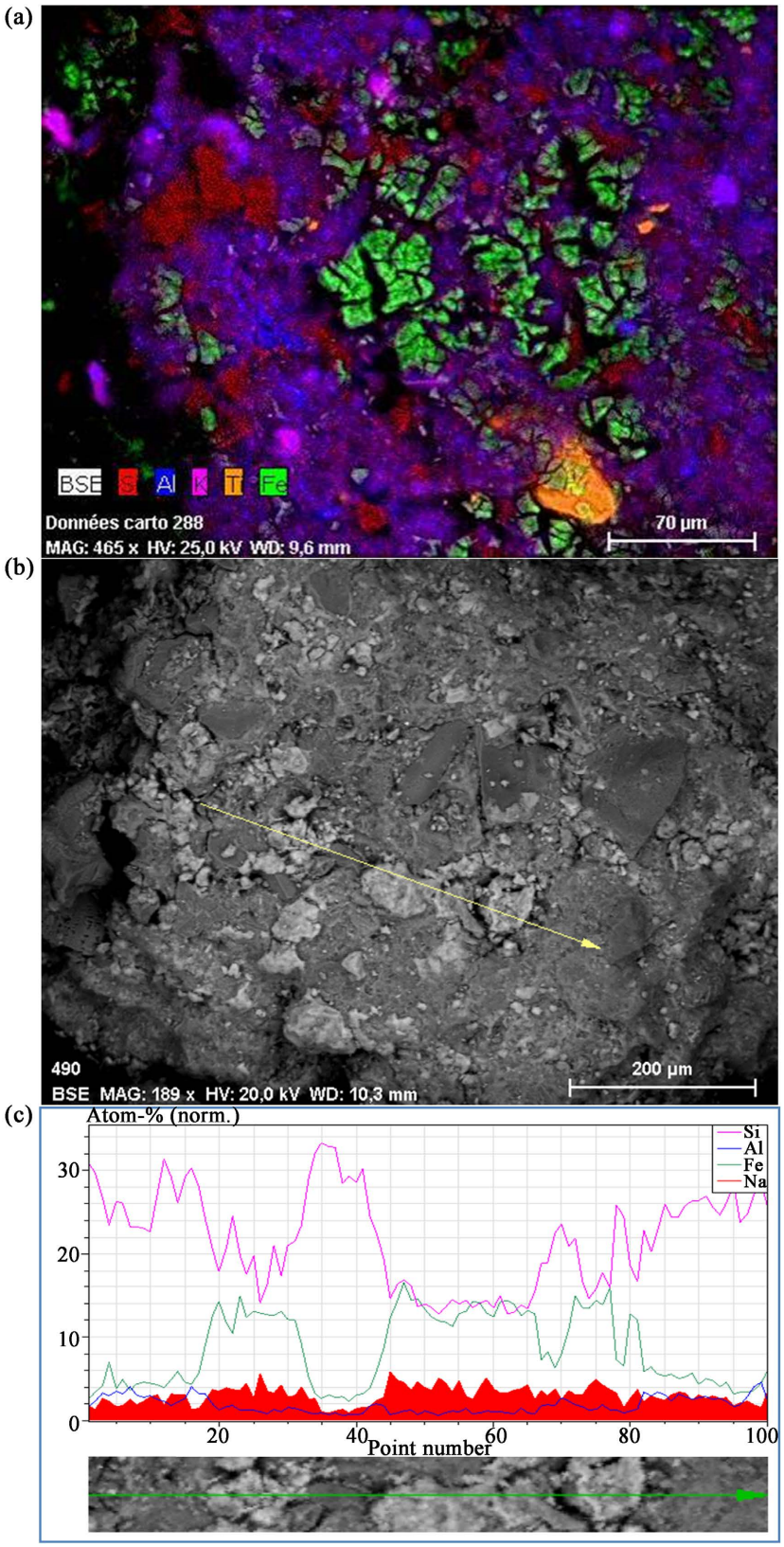

Figure 2. (a) SEM/EDS mapping; (b) SEM/EDS mapping; (iron oxyhydroxide: green, Aluminum blue; Silicium red) (c) SEM image of the surface of brick grains rich in iron oxyhydroxides.

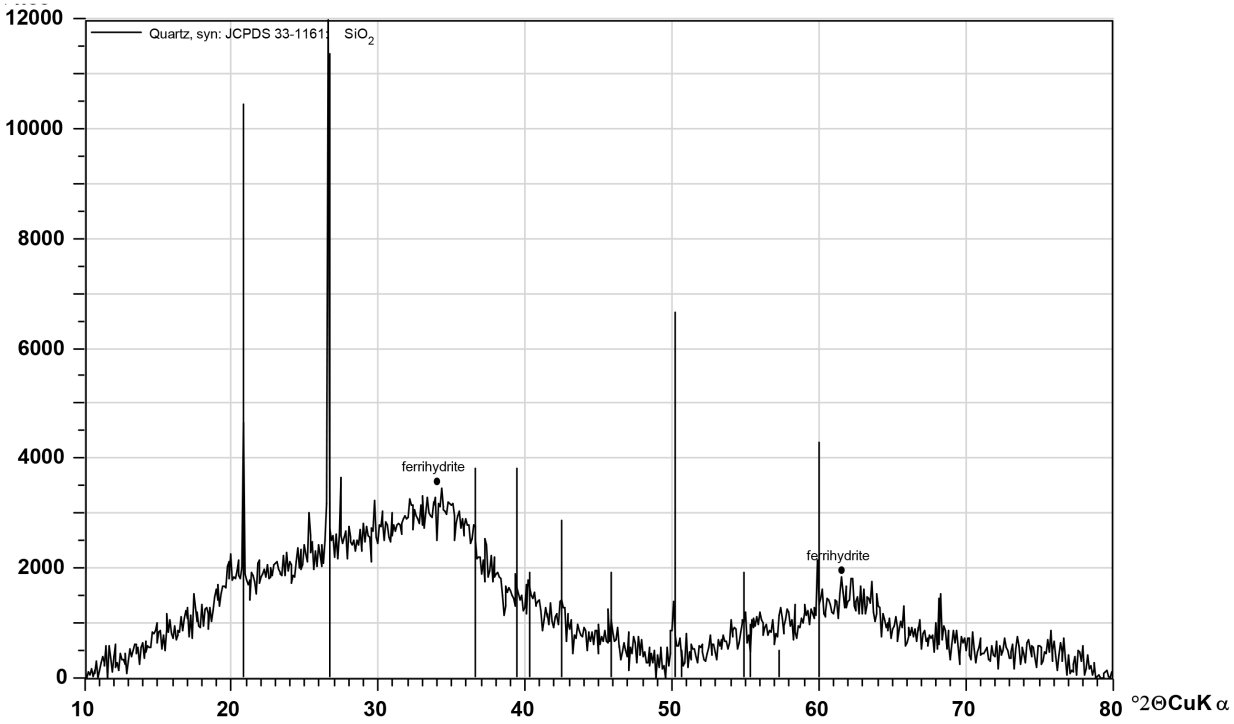

Figure 3. RX diffractogram of a brick sample after deposition of ferrihydrite (anticathode of Cu Kα1, λ = 1.54060 Å exposure 7 h).

$$Q_{total} = \frac{F}{1000}\int_{t=0}^{t=t_{total}} \left(C_{ads}\mathrm{d}t\right) \tag{1}$$

where Q_{total} is the maximum quantity of iron(II) adsorbed by the fixed bed (mg), F is the flow rate (mL·min^{-1}), C_{ads} is the adsorbed iron(II) concentration (mg·L^{-1}) and t is the time (min).

The maximum capacity of the column fixed bed was calculated using Equation (2).

$$Q_{\max} = \frac{Q_{total}}{m_{brick}} \tag{2}$$

where m_{brick} represented the total dry weight of ferrihydrite-coated brick inside the column.

Total removal percent of iron(II) of the column fixed bed was defined using Equation (3)

$$Y\% = \frac{Q_{total}100}{m_{solute}^{total}} \tag{3}$$

where is the total amount of iron(II) passed through the column during the experiment, it was calculated from the Equation (4):

$$m_{solute}^{total} = \frac{C_0 F t_{total}}{1000} \tag{4}$$

5.1. Effect of Flow Rate

To obtain the fixed bed maximum capacities, the effect of flow rate was investi-

gated at a constant bed height of 15 cm. It can be seen in (Figure 4) the plots of comparative normalized iron(II) concentration, C_t/C_0, against the time passed through a 14 mm diameter column of the modified brick at different flow rates. Also, from the plots in (Figure 4) sorption data were assessed, and particularly, amount of total iron-sorbed, maximum iron uptake per gram of brick and total removal percent with respect to volumetric flow rate are listed in Table 1.

As a whole, it was noticed mainly three features: 1) metal-uptake values remained relatively constant with flow rate (0.338 ± 0.010 mg/g for F = 3 - 10 mL/min); 2) sharper breakthrough curves were obtained at higher flow rates (the $\Delta c/\Delta t$ ratio which is defined in Table 1, varied from 0.069 mg/L min for F = 3

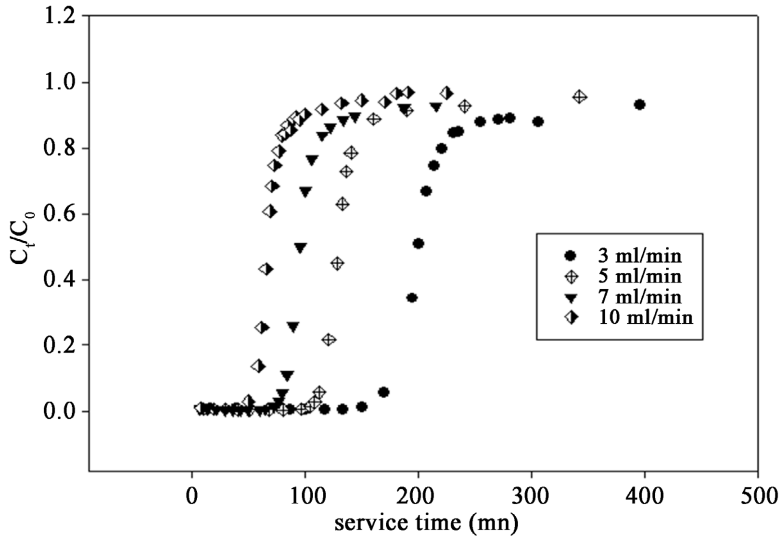

Figure 4. Effect of various flow rates on the breakthrough curve of Fe(II) adsorption on ferrihydrite coated brick at a constant bed depth.

Table 1. Column data and parameters obtained for iron(II) ions adsorption on ferrihydrite coated brick in water at various bed depths and flow rates. The subscripts "b" and "e" corresponded to the words "breakthrough" and "exhaustive".

Bed deph (Z) cm	Brick mass g	Flow rate (F) ml/min	Uptake (Q_{exp}) mg/g	t_b min	V_b ml	$t_{50\%}$ min	t_e min	V_e ml	Δt min	$\Delta (C_t)/\Delta t$ mg/l/min
10	16	10	0.344	33	326	46	80.7	792	48	0.18
15	25	10	0.299	50	504	66	100	1000	50	0.174
		7	0.299	73	507	96	144	1007	71	1.132
		5	0.306	105	522	129	241	1201	136	0.071
		3	0.346	151	452	21	306	915	155	0.069
15	23	10	0.328	50	504	66	100	1000	50	0.174
20	30	10	0.336	78	753	98	132	1278	54	0.162
25	38	10	0.334	110	1008	124	164	1502	54	0.174

mL/min to 0.174 mg/L min for F = 10 mL/min); and 3) the breakpoint time (t_b) decreased with increasing flow rates and at a constant mass of brick inside the column: m = 23.4 $\pm$ 0.4 g (from t_b = 151 min for F = 3 mL/min to t_b = 50 min for F = 10 mL/min). It should further be noted that a better Fe(II) adsorption performance of the study brick was obtained at the lowest flow rates, due to higher residence time.

5.2. Effect of Bed Height

The breakthrough curves of iron(II) adsorption which were obtained in a 14 mm diameter column at different bed heights with a constant flow rate of 10 mL/min are given in (Figure 5). For this column (14 mm diameter), the bed height was about 10, 15, 20 and 25 cm, which corresponded to brick masses of 16, 23, 30, 38 g, respectively.

It was found that a higher bed height or an increase in adsorbent weight inside the column led to higher quantities of adsorbed Fe(II) in the column reported in Table 1, due to the involvement of more adsorption brick sites in interaction with the effluent. Obviously, the maximum capacity of iron-uptake per gram of brick remained relatively constant with increasing bed height (as reported in Table 1). This result could be attributed to the number of up-take sites per gram of brick which remained constant when increasing bed height.

5.3. Evaluation of Basic Design Parameters of Adsorption Column

The time required for the exchange zone to move the length of its own height up/down the column (t_z) once it has become established is [18] [19] [20]:

$$t_z = \frac{V_s}{F} \tag{5}$$

where Vs is the total volume (mL) of water treated between t_b and t_e and F is the

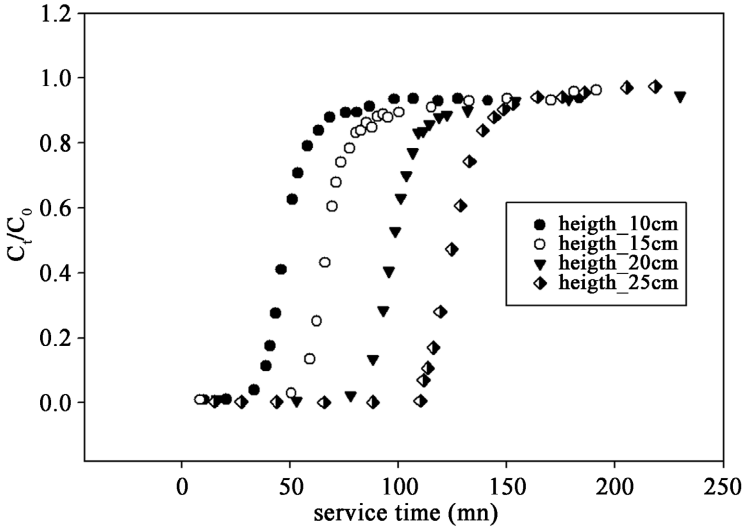

Figure 5. Effect of various bed depths on the breakthrough curve of Fe(II) adsorption on ferrihydrite coated brick at a constant flow rate.

flow rate (mL·min^{-1}).

The time required for the exchange zone to become established and move completely out of the bed (t_e) is:

$$t_e = \frac{V_e}{F} \tag{6}$$

where Ve is the total volume of iron(II) spiked water treated to the point of exhaustion (L).

The rate at which the adsorption zone is moving up and down through the bed is:

$$U_Z = \frac{h_Z}{t_Z} = \frac{h}{t_e - t_f} \tag{7}$$

where h_z is the height of exchange zone (cm); h is the total bed depth (cm); t_f is the time (min) required for the adsorption zone to form initially.

The expression for the height of the exchange zone (h_z) is:

$$h_Z = \frac{h(t_Z)}{t_e - t_f} \tag{8}$$

The value of $t_f$can be calculated as:

$$t_f = (1 - f)t_Z \tag{9}$$

where f is the fraction of iron(II) adsorbed when the adsorption zone is completely saturated after equilibrium, is given by:

$$f = \frac{S_Z}{S_{\max}} = \frac{\int_{V_b}^{V_e}(C_0 - C_t)\mathrm{d}V}{C_0(V_e - V_b)} \tag{10}$$

where C_0 is the initial concentration of iron(II) in water (mg/L); C_t is the concentration of solute iron(II) at any instant in the effluent (mg/L); V_b is the total volume of iron(II) spiked water treated to the point of breakthrough (L); S_z is the amount of iron(II) that has been removed by the adsorption zone from breakthrough to exhaustion (mg) and $S_{\max}$ is the amount of iron(II) removed by adsorption zone if completely exhausted (mg).

The percentage of total column bed saturated at breakthrough is:

$$\%saturation = \frac{h + (f - 1)h_Z}{h} \times 100 \tag{11}$$

It was noted that the moving rate of the exchange zone (U_Z) increases with the flow rate. U_Z ranges from 0.072 to 0.214 cm/min when the flow rate increases from 3 to 10 ml/min (**Table 2**). These values are in agreement with the experimentally determined ratio $\Delta(C_t)/\Delta t$ which decreases with the flow rate. On the other hand, it shows in **Table 2** that the height of the exchange zone remains almost constant at all the rates of the filtration. Therefore it was found that the exchange zone does not depend on the height of the fixed bed and the filtration rate but probably on the affinity of the solute with the adsorbent. The variation

Table 2. Design Parameters for fixed bed column applied to Fe^{2+} ions adsorption on ferrihydrite coated brick in water at various bed depths and flow rates.

Bed depth cm	Flow rate (F) ml/min	U_Z cm/min	t_z min	h_z cm	t_f min	t_e min	% saturation
10	10	0.2	46.6	9.3	29.2	79.2	41.59
15	3	0.072	154.12	11.03	95.39	304.92	54.47
	5	0.112	84.77	9.45	54.65	189.14	59.36
	7	0.149	71.53	10.65	43.17	143.91	57.15
	10	0.214	49.66	10.63	29.96	100.02	57.23
15	10	0.210	49.600	10.600	30.0	100.000	57.230
20	10	0.21	52.5	10.8	30.7	127.8	68.29
25	10	0.21	49.4	10.4	31.6	150.2	73.31

of the percentage of saturation as a function of the flow rate is not significant to affirm an influence of the variation of flow rate on the height of the exchange zone.

The mathematical evaluation of the basic adsorption column design parameter using various bed heights permitted us to show that the moving of the adsorption zone in the adsorbent bed is independent of the bed height and remained constant (U_Z = 0.208 ± 0.006) cm/min when increasing bed height. The values of U_Z are close to those experimentally obtained for the ratio $\Delta(C_t)/\Delta t$ between the breakthrough time (t_b) and the exhaustive time (t_e). This ratio also remains constant and equals 0.17 ± 1 mg/l/min and corresponds to the variation of the concentration of iron(II) adsorbed on the support per unit of time.

It was found when the bed heights of column increased to 10 from 25 cm, the height of the exchange zone in the column also remains constant, h_Z = 10.3 ± 0.6 cm.

The time required for the adsorption zone to move vertically up the column (t_Z) and the time required for the adsorption zone to become totally saturated were also constant (see Table 2), in agreement with the moving rate and the height of the adsorption zone which were invariable when the heights of column bed varied from 10 to 25 cm Between the breakthrough time (t_b) and the exhaustive time (t_e) when the heights of column bed varied to 10 from 25 cm, the percentage of the total column saturation at breakthrough varied from 41.59 to 73.31. This increase of the saturation percentage is in agreement with the theoretical data from Equation (3).

5.4. Prediction of Service Times of Columns, Using the BDST and Comparison with the Experimentally Obtained Service Times

Bed Depth Service Time (BDST)

A number of mathematical models have been developed for use in design. Some

investigators attempted to simulate column performances by testing mathematical models from data collected during laboratory experiments in order to design pilot-scale columns [21] [22] [23] with mathematical models. Among them, differential Bohart-Adams equations [18] [24] [25] were successfully applied to liquid-solid systems by accounting for the dynamics of the study adsorption process. Briefly, the decrease with time of the adsorption capacity, "No", of the adsorbent was found to be proportional to the adsorption rate, K_{ads}, as follows:

$$\frac{\partial N_0}{\partial t} = k_{ads} N_0 C \tag{12}$$

Hutchins [26] proposed a simplified equation based on the above surface-reaction-rate theory proposed by Bohart and Adams (1920): it was presented as a linear relationship between the column bed depth (Z (cm)) and the service time (t (min)):

$$t = \frac{N_0}{C_0 \upsilon} Z - \frac{1}{k_{ads} C_0} \ln\left(\frac{C_0}{C_t} - 1\right) \tag{13}$$

where N_0 represented the dynamic bed capacity (mg/L); ν was the linear flow rate (cm/min) which was defined as the ratio of the volumetric flow rate F (cm^3/min) to the cross-sectional area of the bed, S (cm^2); K_{ads}. was the adsorption rate constant (L/mg min); and C_0 and C_t corresponded to the influent Fe^{2+} concentration and the effluent Fe^{2+} concentration at time t, respectively.

At a time ($t_{50\%}$) at which Fe(II) concentration in the effluent reached 50% of the influent Fe(II) concentration, BDST Equation (14) can be simplified as:

$$t_{50\%} = \frac{N_0 Z}{C_0 \upsilon} \tag{14}$$

The critical column height (Z_0) is the minimum column height necessary to produce $C_t < C_{5\%}$ of the initial concentration of the effluent.

The time $t = 0$ was determined in Equation (13).

$$Z_0 = \frac{\upsilon}{k_{ads} N_0} \ln\left(\frac{C_0}{C_{0.05}} - 1\right) \tag{15}$$

During the experiments, three particular values of the service time were studied: t_b, $t_{50\%}$ and t_e, which correspond to 5%, 50%, and 90% of initial concentration in the effluent at the outlet of the column. The variation of these three service times V_s the height of the bed column permitted us to get three lines in agreement with the Hutchins equation (**Figure 6**). Which showed the depth vs service time for t_b = 0.5%, $t_{50\%}$ = 50% and t_e = 90% saturation of the columns. The equations and correlation coefficients of these lines are as follows:

$$t_b = 5.18Z - 22.9, \quad R^2 = 0.98 \tag{16}$$

$$t_{50\%} = 5.38Z - 7, \quad R^2 = 0.98 \tag{17}$$

$$t_e = 5.62Z + 20.9, \quad R^2 = 0.98 \tag{18}$$

From the slopes these lines t_b and t_e are parallel and the horizontal distance

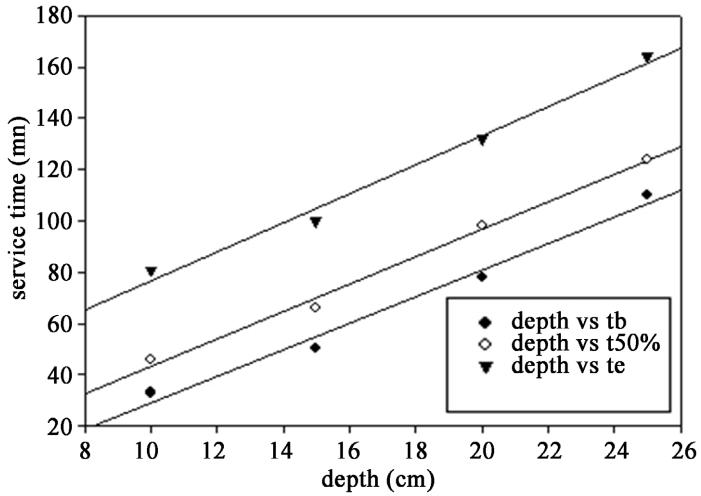

Figure 6. Bed depth vs service time plot at 5%, 50% and 90% saturation of ferrihydrite coated brick fixed bed.

between the lines was found to be 10.71 cm. This horizontal distance is the height of the exchange zone in agreement with theoretically value that was averaged to be 10.3 ± 0.6 cm (**Table 2**).

The slopes of these 3 lines are similar and allow from Equation (13) to calculate from the 3 times (t_b, $t_{50\%}$ and t_e) an average value of dynamic capacity N_0: 345 ± 15 mg/L. The minimum column height (Z_0) necessary to produce an effluent concentration of C_t < C5% was showed in **Table 3**. It can be seen Z_0 remained nearly constant at a given flow rate of 10 mL/min and at bed height varying from 10 to 25 cm. This meant that Fe(II) adsorption onto brick pellets ought to be efficient only if studied bed heights Z was $>Z_0$.

From this value N_0, the adsorption constant K_{ads} can be reached. This constant calculated from the different times t_b increases slightly with the height of the bed (**Table 3**). The reason for weak increases observed for K_{ads} might be due to physical column parameters like wall effects.

By plotting the variations of t_b, $t_{50\%}$, and t_e Vs $1/\upsilon$ with the υ was a linear rate in cm/min of liquid flow calculated from the flow rate (**Figure 7**).

$$t_e = 304.75x + 3.351, \quad R^2 = 0.92 \tag{19}$$

$$t_{50\%} = 405.8x + 1.2612, \quad R^2 = 0.99 \tag{20}$$

$$t_b = 625.39x + 9.8837, \quad R^2 = 0.98 \tag{21}$$

Regression coefficient values: show that the results obtained are well representative of Equation (14). From the slope and the intercept these parameters N_0, K_{ads} and Z_0 were calculated and shown in **Table 3**.

By taking into account the values of the initial concentration and linear rates of filtration, the dynamic bed capacity was found to be N_0 = 335 mg/l. This value is very close to N_0 obtained by varying the height of the bed, *i.e.* N_0 = 345 mg/l. The adsorption rate constant K_{ads} does not change significantly with the rate and is 32.4 ± 2 mL/(mg/min). The critical bed depth, Z_0, increased from 0.83 to 3.25

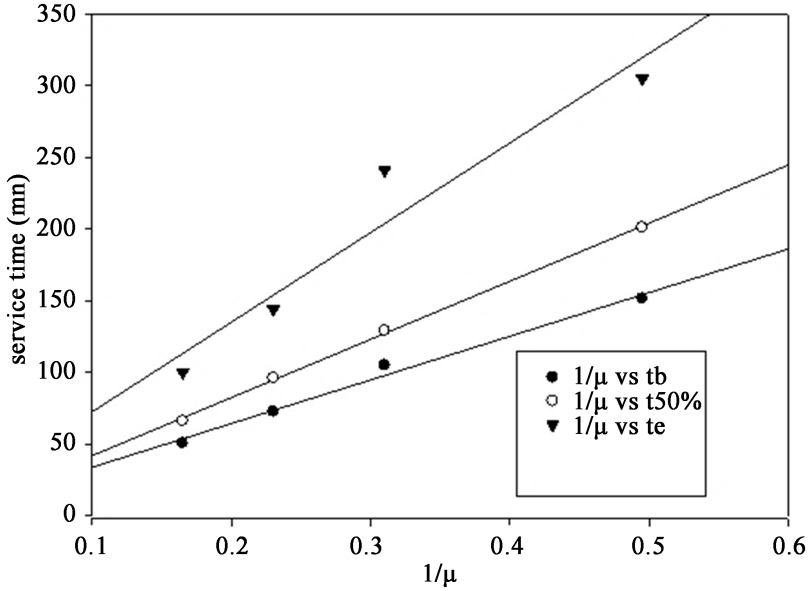

Figure 7. Flow rate vs service time plot at 5%, 50% and 90% saturation of ferrihydrite coated brick fixed bed.

Table 3. Parameters predicted from BDST model applied to Fe^{2+} ions adsorption on ferrihydrite coated brick in water at various bed depths and flow rate.

Bed depth (h) cm	Brick mass (m) g	Flow rate (F) ml/min	N_0 mg/L	K_{ads} mL/(mg min)	Z_0 cm	R^2
10	16	10	345	16.3	3.96	0.988
15	23.0	10	335	30	3.25	0.999
	23.8	7	335	34.1	1.7	
	23.1	5	335	33.9	1.19	
	23.1	3	335	31.5	0.89	
15	23	10	345	17.8	4.04	0.988
20	30	10	345	19.2	3.92	
25	38	10	345	25.8	3.88	

cm with increased flow rate from 3 to 10 mL/min at a given bed height of 15 cm. The Fe(II) adsorption onto brick was efficient because bed heights $Z > Z_0$.

To compare, the experimental data shows that the values of height of the exchange zone was in agreement with theoretical data using BDST model. Both curves revealed a good correlation for the treated iron system.

6. Conclusion

In this study, an investigation was carried out in the laboratory to evaluate the Fe(II) adsorption on ferrihydrite-coated brick in fixed bed column. Microscopic analyses (ESEM/EDS) of this adsorbent were carried out and its data permitted

us to show the ferrihydrite bound to surface brick and identified as two-line ferrihydrite by XRD as the key adsorbent in the process. Our finding further revealed that these natural brick materials could also be used efficiently for Fe(II) removal. It was found that the Fe(II) adsorption was to be dependent upon the flow rate and bed depth in fixed bed columns. However, the basic parameters such as 1) moving rate of exchange zone increases when increasing the flow rate in the bed column and does not depend on column bed heights, 2) the height of exchange zone remains constant when increasing the flow rate and the bed height. The BDST model was used to evaluate the column capacity, and breakthrough data predictions and the evaluation of the column parameters gave results that showed good agreement with experimental results., These adsorptive properties should be explored for water-treatment technologies at low cost in Central African Republic since brick is easily available and cheap in this country.

Acknowledgements

This study is partly funded by the "Agence de l'Eau Artois-Picardie", the "Region Nord Pas-de-Calais", and the "city of Villeneuve d'Ascq". These investigations were undertaken successfully owing to the cooperation between the University of Lille1 (France) and the University of Bangui (Central African Republic). This collaboration (being still underway) and the Grant-in-Aid to Mr. O. Allahdin in a post-doctoral position have been financially supported by the Embassy of France to Bangui.

Conflicts of Interest

The authors declare no conflicts of interest regarding the publication of this paper.

References

[1] Chaturvedi, S. and Dave, P.N. (2012) Removal of Iron for Safe Drinking Water. *Desalination*, **303**, 1-11. https://doi.org/10.1016/j.desal.2012.07.003

[2] El Azher, N., Gourich, B., Vial, C., Belhaj Soulami, M. and Ziyad, M. (2008) Study of Ferrous Iron Oxidation in Morocco Drinking Water in an Air Lift Reactor. *Chemical Engineering and Processing*, **47**, 1877-1886. https://doi.org/10.1016/j.cep.2007.10.013

[3] Mohan, D. and Chander, S. (2006) Removal and Recovery of Metal Ions from Acid Mine Drainage Using Lignite—A Low Cost Sorbent. *Journal of Hazardous Materials B*, **137**, 1545-1553. https://doi.org/10.1016/j.jhazmat.2006.04.053

[4] Dehou, S.C., Wartel, M., Recourt, P., Revel, B., Mabingui, J., Montiel, A. and Boughriet, A. (2012) Physicochemical, Crystalline and Morphological Characteristics of Bricks Used for Ground Waters Purification in Bangui Region (Central African Republic). *Applied Clay Science*, **59-60**, 69-75. https://doi.org/10.1016/j.clay.2012.02.009

[5] Lee, S.M., Laldawngliana, C. and Tiwari, D. (2012) Iron Oxidenano-Particles—Immobilized-Sand Material in the Treatment of Cu(II), Cd(II), and Pb(II) Contaminated Waste Waters. *Chemical Engineering Journal*, **195-196**, 103-111.

https://doi.org/10.1016/j.cej.2012.04.075

[6] Katsoyiannis, I.A. and Zouboulis, A.I. (2002) Removal of Arsenic from Contaminated Water Sources by Sorption onto Iron-Oxide-Coated Polymeric Materials. *Water Research*, **36**, 5141-5155. https://doi.org/10.1016/S0043-1354(02)00236-1

[7] Eren, E. and Gumus, H. (2011) Characterization of the Structural Properties and Pb(II) Adsorption Behavior of Iron Oxide Coated Sepiolite. *Desalination*, **273**, 276-284. https://doi.org/10.1016/j.desal.2011.01.004

[8] Hua, M., Zhang, S., Pan, B., Zhang, W., Lv, L. and Zhang, Q. (2012) Heavy Metal Removal from Water/Wastewater by Nanosized Metal Oxides: A Review. *Journal of Hazardous Materials*, **211**-**212**, 317-331. https://doi.org/10.1016/j.jhazmat.2011.10.016

[9] Boujelben, N., Bouzid, J. and Elouear, Z. (2009) Adsorption of Nickel and Copper onto Natural Iron Oxide-Coated Sand from Aqueous Solutions: Study in Single and Binary Systems. *Journal of Hazardous Materials*, **163**, 376-382. https://doi.org/10.1016/j.jhazmat.2008.06.128

[10] Mohan, D. and Pittman Jr., C.U. (2007) Arsenic Removal from Water/Wastewater Using Adsorbents—A Critical Review. *Journal of Hazardous Materials*, **142**, 1-53. https://doi.org/10.1016/j.jhazmat.2007.01.006

[11] Boujelben, N., Bouzid, J., Elouear, Z., Feki, M., Jamoussi, F. and Montiel, A. (2008) Phosphorus Removal from Aqueous Solution Using Iron Coated Natural and Engineered Sorbents. *Journal of Hazardous Materials*, **151**, 103-110. https://doi.org/10.1016/j.jhazmat.2007.05.057

[12] Dehou, S.C. (2011) Etude des propriétés d'adsorption des oxyhydroxydes de fer déposés sur un support naturel (la brique): Application à l'élimination du fer dans les eaux de forages en République Centrafricaine. Thesis, University of Lille 1, Lille, 157.

[13] Allahdin, O., Dehou, S.C., Wartel, M., Recourt, P., Trentesaux, M., Mabingui, J. and Boughriet, A. (2013) Performance of FeOOH-Brick Based Composite for Fe(II) Removal from Water in Fixed Bed Column and Mechanistic Aspects. *Chemical Engineering Research and Design*, **91**, 2732-2742. https://doi.org/10.1016/j.cherd.2013.04.006

[14] Dehou, S.C., Wartel, M., Recourt, P., Revel, B. and Boughriet, A. (2012) Acid Treatment of Crushed Brick (from Central African Republic) and Its Ability (after FeOOH Coating) to Adsorb Ferrous Ions from Aqueous Solutions. *The Open Materials Science Journal*, **6**, 50-59. https://doi.org/10.2174/1874088X01206010050

[15] Dehou, S.C., Mabingui, J., Lesven, L., Wartel, M. and Boughriet, A. (2012) Improvement of Fe(II)-Adsorption Capacity of FeOOH-Coated Brick in Solutions, and Kinetics Aspects. *Journal of Water Resource and Protection*, **4**, 464-473. https://doi.org/10.4236/jwarp.2012.47054

[16] Allahdin, O., Wartel, M., Mabingui, J. and Boughriet, A. (2015) Surface Characteristics of the Iron-Oxyhydroxide Layer Formed during Brick Coatings by ESEM/EDS, 23Na and 1H MAS NMR, and ToF-SIMS. *American Journal of Analytical Chemistry*, **6**, 11-25. https://doi.org/10.1016/j.matchemphys.2015.09.021

[17] Bohart, G.S. and Adams, E.Q. (1920) SOME Aspects of the Behavior of Charcoal with Respect to Chlorine. *Journal of the American Chemical Society*, **42**, 523. https://doi.org/10.1021/ja01448a018

[18] Stumm, W. and Morgan, J.J. (1996) Aquatic Chemistry: Chemical Equilibria and Rates in Natural Waters. Third Edition. Environmental Science and Technology. John Wiley & Sons, New York, 461.

[19] Kundu, S. and Gupta, A.K. (2005) Analysis and Modeling of Fixed Bed Column Operations on As(V) Removal by Adsorption onto Iron Oxide-Coated Cement (IOCC). *Journal of Colloid and Interface Science*, **290**, 52-60. https://doi.org/10.1021/ja01448a018

[20] Brion-Roby, R., Gagnon, J., Deschênes, J.-S. and Chabot, B. (2018) Investigation of Fixed Bed Adsorption Column Operation Parameters Using a Chitosan Material for Treatment of Arsenate Contaminated Water. *Journal of Environmental Chemical Engineering*, **6**, 505-511. https://doi.org/10.1016/j.jece.2017.12.032

[21] Allahdin, O. (2014) Elimination (par adsorption sur la brique activée) de polluants métalliques dans les eaux de la République Centrafricaine et les pays en voie de développement. Aspects texturaux, physico-chimiques (électro)cinétiques et thermodynamiques. Thesis, University of Lille 1, Lille, 61-63.

[22] Sharma, D.C. and Forster, C.E. (1996) A Comparison of the Sorbtive Characteristics of Leaf Mould and Activated Carbon Columns for the Removal of Hexavalent Chromium. *Process Biochemistry*, **31**, 213-218. https://doi.org/10.1016/0032-9592(95)00049-6

[23] Sarin, V., Singh, T.S. and Pant, K.K. (2006) Thermodynamic and Breakthrough Column Studies for the Selective Sorption of Chromium from Industrial Effluent on Activated Eucalyptus Bark. *Bioresource Technology*, **97**, 1986-1993. https://doi.org/10.1016/j.biortech.2005.10.001

[24] Malkoc, E. and Nuhoglu, Y. (2006) Cr(VI) Adsorption by Waste Acorn of *Quercus ithaburensis* in Fixed Beds: Prediction of Breakthrough Curves. Y. Abali. *Chemical Engineering Journal*, **119**, 61-68. https://doi.org/10.1016/j.cej.2006.01.019

[25] Sahel, M. and Ferrandon-Dusart, O. (1993) Adsorption Dynamique en Phase Liquide sur Charbon Actif: Comparaison et simplification de différents modèles. *Water Science*, **6**, 63-80. https://doi.org/10.7202/705166ar

[26] Vijayaraghavan, K. and Prabu, D. (2006) Potential of *Sargassum wightii biomass* for Copper(II) Removal from Aqueous Solution: Application of Different Mathematic Models to Batch and Continuous Biosorption Data. *Journal of Hazardous Materials B*, **137**, 558-564. https://doi.org/10.1016/j.jhazmat.2006.02.030